VirtualBrainCloud

Personalized Recommendations for Neurodegenerative Disease

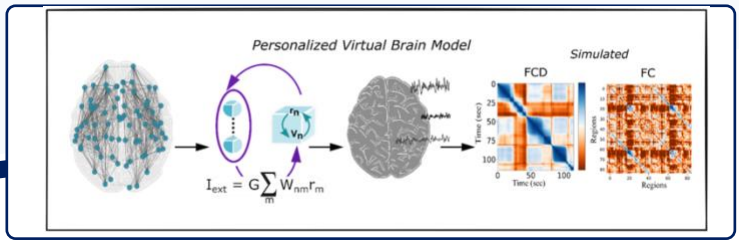

www.VirtualBrainCloud-2020.eu

Public deliverable report

D8.2: Individualized TVB human models in neurodegenerative disease

Date May 2023

Authors Jan Fousek, Meysam Hashemi, Abolfazl Ziaee Mehr, Viktor Jirsa
(Aix-Marseille Université)

Dissemination level: **public**
Website www.VirtualBrainCloud-2020.eu

This project has received funding from the **European Union´s Horizon 2020** research and innovation programme under **grant agreement No 826421**

Table of content

1. Introduction

The VirtualBrainCloud (TVB-Cloud) has developed a cloud-based brain simulation platform to support development, implementation and application of diagnostics and interventions in the context of neurodegenerative diseases (NDD). At the core, these workflows make the link between simulated and empirical data for each individual patient and relate it to the structural and functional alterations in NDD. In this deliverable we provide an instantiation of such a link in the case of Alzheimer's disease (AD), and make available the corresponding individualized TVB human models.

AD is a neurodegenerative disorder characterized by the accumulation of abnormal beta-amyloid (Aβ) and hyperphosphorylated Tau (pTau) with specific spatial and temporal pattern of progression (Braak & Braak, 1991). This accumulation is accompanied by changes in neuronal activity, among others characterized by increased excitability of the affected neuronal populations (Roberson et al., 2007; Ittner et al., 2010; DeVos et al., 2013), however disentangling the effects on the network level is challenging. Modeling approaches on the whole-brain level (Ghosh et al., 2008; Deco et al., 2011; Sanz Leon et al. , 2013; Breakspear, 2017; Bassett et al., 2018) have the capacity to characterize the relationship between brain anatomy, physiology and brain dynamics, allowing for exploration of causal effects. For AD, the disease driven hyper-activity was explored as link between local and global dynamics (Zimmermann et al., 2018; Stefanovski et al., 2021; Triebkorn et al., 2022; Arbabyazd et al., 2021; Patow et al., 2022). Here we take the next step, and turn to model inversion as a strategy to infer the hidden causes (D'Angelo and Jirsa, 2022) while quantifying the uncertainty and test alternative hypotheses within the framework of Bayesian inference (Friston 2010, Hashemi et al., 2020).

The approach presented here (Yalçınkaya et al., 2023) takes full advantage of the individualized whole-brain modeling and inference framework applied on a cohort level. As a first step, a battery of empirical data features is established to capture the changes in the brain structure (e.g. connectivity) and function (resting state), in this case lifted from the MRI measurements. Cohort-level trends are then identified with respect to these data features, and in the next step, combined with the prior domain knowledge to formulate mechanistic hypothesis on how the structural changes express themselves in the brain function along the disease trajectory. Next, the identifiability of relevant parameters is evaluated on synthetic data with the known ground truth which is produced from the individualized brain models to aid the development of reliable inference workflow. And lastly, the workflow is validated on the empirical data. The implementation employs the tools and software of the TVB-inversion presented in deliverable D8.1[1].

In this deliverable we present a personalization workflow based on region specific changes related to disease progression, here specifically the level of excitability in the limbic system. When mechanistically implemented in personalized brain models, simulations demonstrate the causal changes in the functional brain dynamics quantified by a battery of metrics, including functional connectivity and fluidity (functional connectivity dynamics) of the resting state activity. Empirical data from the Sydney Memory and Ageing Study (MAS) were used to derive the cohort-level trends and validate the inference workflow. In addition, the individual virtual brain models are made available together with the estimated parameters.

[1] D8.1: Validated and benchmarked data fitting workflow will be provided as a software for brain model personalization

2. Partners involved

AMU

3. Work performed and Results

3.1. Empirical data features

The subjects for this study were selected from the Sydney Memory and Aging Study (MAS) (Sachdev et al., 2010; Tsang et al., 2013), and stratified into three groups based on cognitive performance: 71 healthy controls (HC), 32 with amnestic mild cognitive impairment (aMCI), and 12 with Alzheimer's disease (AD). For each of the subjects, magnetic resonance imaging (MRI) data (resting state functional MRI (rs-fMRI) and diffusion MRI (dMRI)) were preprocessed and structural connectivity (SC) and region-average fMRI (BOLD signal) were computed using the AAL Atlas (Zimmerman et al., 2018). On this data, a battery of data features was evaluated with respect to differences between healthy and cognitively declined subjects. In particular, the functional data features reflected the characteristic changes in functional organization of the AD such as the strength of the homotopic functional connectivity (FC) or time-variant FC dynamics (FCD).

In terms of structural connectivity, the cognitively declined group showed changes only in the limbic network. The whole-brain connectivity, connectivity within and between other lobes, and interhemispheric connections didn't show significant differences. As for the functional changes, we have identified a significant decline in homotopic links in the functional connectivity, and also in the limbic system decrease in an index of fluidity – the variability of FC in time – derived from FCD.

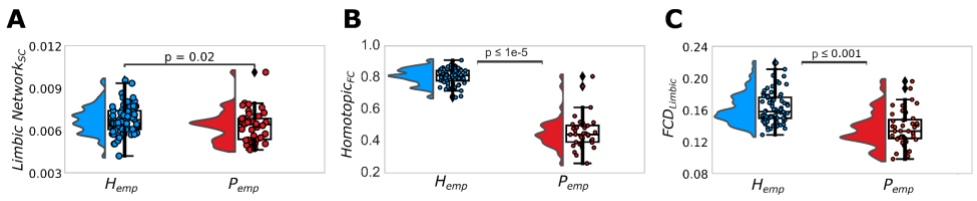

Figure 1: Differences in the structural and functional data features between the healthy subjects (H_{emp}) and cognitively declined (P_{emp}). For structural connectivity, only the strength of connections within the limbic network showed significant difference (A). Out of functional data features, there were significant differences in homotopic functional connectivity (B), and fluidity (variability) of the functional connectivity dynamics within the limbic system(C).

3.2. Exploration of structural degradation vs functional changes

Individual brain models were constructed using the SC for each subject equipped with a neural mass model to govern the activity of each node (Montbrió et al., 2015). Two parameters of the model will be relevant in what follows: the excitability η_i of each node i, and the scaling of the coupling between the nodes with respect to the local dynamics G. This model is then used to generate simulated resting state data on the neural source level, which then were turned into synthetic BOLD signals using the appropriate observer model.

In this model, we investigated three possible mechanisms for the empirically observed group differences in functional data features. We considered following scenarios: a) the personalized connectome for each individual subject (Fig 2: A, B), b) personalized connectome with attenuation of within and outgoing connections of limbic network in the cognitively declined (Fig 2: C, D), and c) personalized connectomes with increased excitability in the limbic regions (Fig 2: E, F). Out of these scenarios, we observed significant effect in the functional data features applied to the simulated data only in the case c) where excitability of the limbic region was considered.

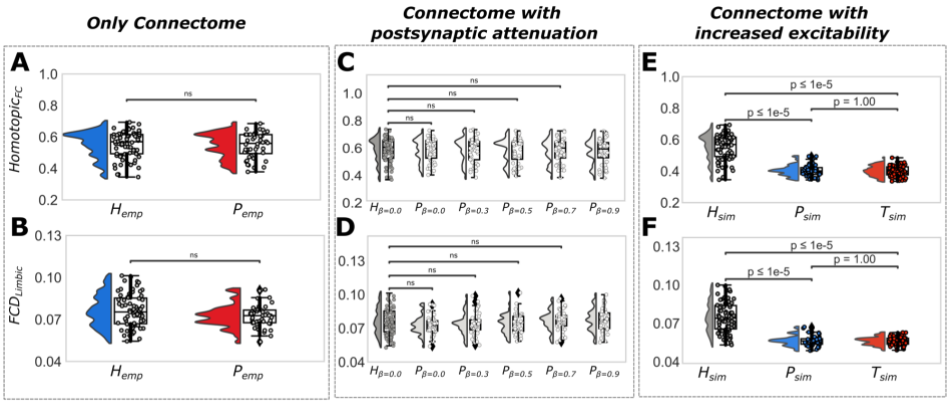

Figure 2: Comparison in-silico of the possible mechanisms underlying the changes in the data features between the groups: homotopic FC (A, C, E), and the fluidity of the FCD within the limbic system (B, D, F). The first scenario considers only the individualized connectomes (A, B) and shows no significant difference. The second scenario adds postsynaptic attenuation, also without significant differences across the gradual increase of the effect (C, D). In the third scenario the excitability of the limbic nodes is altered on top of the individualized connectomes, which leads to significant differences (E, F).

3.3. Parameter identifiability

Simulation-based inference (SBI) allows for Bayesian model inversion using simulated samples from a complex model (Cranmer et al., 2020), and was implemented in the TVB-inversion package introduced in D8.1. Here we use it to infer the global coupling strength scaling G and the excitability η of the nodes belonging to the limbic system. To validate the approach, we first applied it to the synthetic data with known values to demonstrate that SBI can recover accurately the joint posterior distribution of these two parameters.

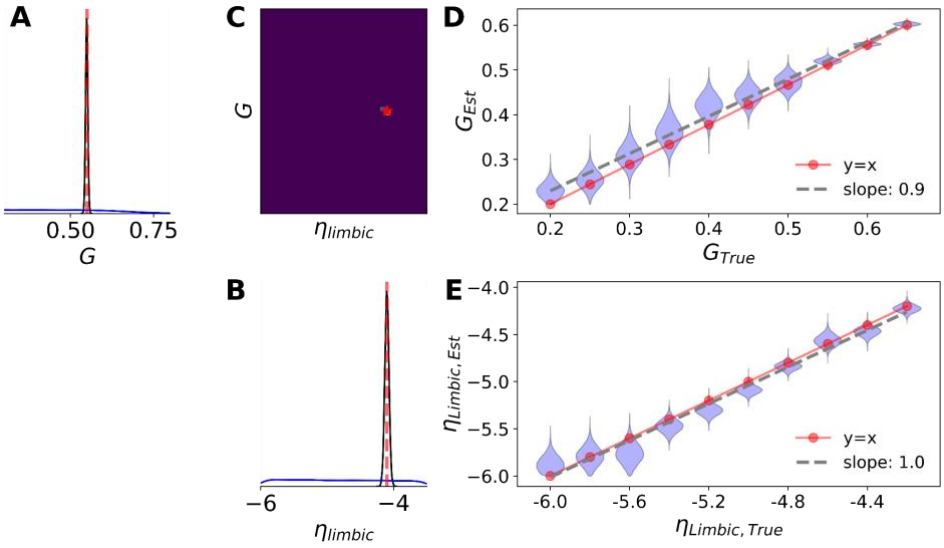

Figure 3: Identifiability of the two parameters evaluated on synthetic data with known ground truth. Inferred posterior distribution of the global coupling scaling (A) and excitability of the limbic regions (B) show shrinkage with respect to the prior distribution (blue), visible also on the joint distribution plot (C). The inferred posterior distributions accurately encompass the true values (red dots) across the range of the ground truth values (D, E).

3.4. Model personalization

Lastly, we applied the SBI to the empirical data using the model formulation detailed above, homotopic FC strength and limbic FCD fluidity index as data features to infer the excitability η and global coupling strength G. The resulting inferred values of the parameter η were significantly increased for the cognitively declined group, whereas G showed nonsignificant decrease. The diagnostic values of posterior shrinkage for both parameters indicate that the posterior distributions were well-identified.

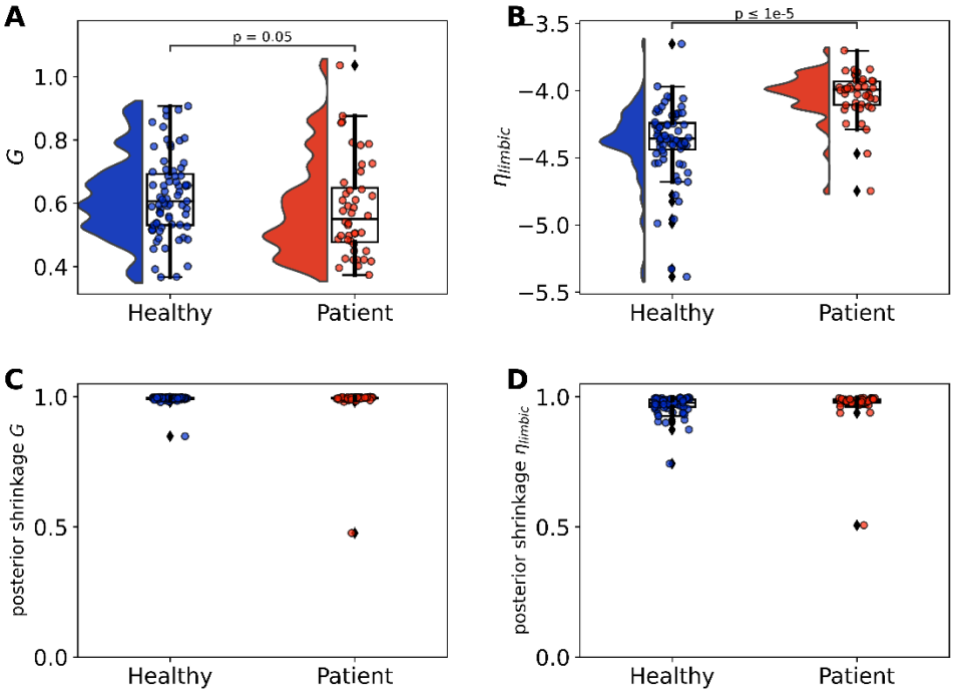

Figure 4: Model parameters inferred for the individual subjects. The inferred values for the global coupling scaling (A) didn't show a significant difference between the groups, while the excitability of the limbic regions (B) did. Both parameters show posterior shrinkage close to 1.0 for all subjects indicating that the posterior is well defined (C, D).

3.5. TVB dataset

We provide the source data and personalized models as a complete dataset. For each of the 115 subjects the empirical MRI derivatives are provided, namely the structural connectivity and the resting state BOLD time series. Complete model definition shared for the cohort is augmented with inidividualized parameters for the global coupling strength G and the excitability of the limbic regions η. Sample codes demonstrating usage in TVB accompany the data to simplify reuse.

The dataset has the following structure:

```
├── CHANGES
├── dataset_description.json
├── model_parameters.json
├── parcellation.txt
├── participants.tsv
├── README
├── SC
│   ├── 0302A
│   │   └── Structural_matrix_0302A.npz
│   ...
├── TS
│   ├── 0302A
│   │   ├── Bold_0302A.npz
│   │   ├── ROICorrelation_0302A.mat
│   │   ├── ROICorrelation_FisherZ_0302A.mat
```

```
│   │   └── ROISignals_0302A.mat
│   ...
├── TVB
│   ├── 0302A
│   │   └── 0302A_connectivity.zip
│   ...
```

Figure 5: Dataset structure overview.

Here the SC folder contains the connectivity matrices for each subject, TS folder contains the BOLD time-series and connectivity matrices, and the TVB folder provides the connectivity matrices in the TVB file format. The individualized model parameters G and η_{limbic} are given in the `participants.tsv` table.

The dataset is available upon request.

4. Conclusion, next steps

The results presented here together with the cohort of personalized TVB models offer several directions for the next steps. First, the results presented here may be efficiently validated in additional suitable cohorts (such as ADNI). Second, to increase findability of the dataset, it will be registered in the publicly searchable data indexes such as the EBRAINS Knowledge Graph. And lastly, extending the personalization workflow for the AD to other functional modalities such as electro- or magneto-encephalograms, seems promising given the converging evidence of disrupted excitation-inhibition balance as one of the early hallmarks of AD.

5. References

Arbabyazd, L., Shen, K., Wang, Z., Hofmann-Apitius, M., Ritter, P., McIntosh, A. R., … & Jirsa, V. Virtual connectomic datasets in Alzheimer's Disease and aging using whole-brain network dynamics modelling. Eneuro, 8(4) (2021).

Bassett, D. S., Zurn, P., & Gold, J. I. On the nature and use of models in network neuroscience. Nat. Rev.Neurosci. 19(9), 566–578 (2018).

Braak, H. & Braak, E. Neuropathological stageing of Alzheimer-related changes. Acta Neuropathol. 82, 239–259 (1991).

Breakspear, M. Dynamic models of large-scale brain activity. Nat. Neurosci. 20(3), 340–352 (2017).
DeVos, S. L. et al. Antisense reduction of tau in adult mice protects against seizures. J Neurosci. 33, 12887-97 (2013).

Deco, G., Jirsa, V. K., & McIntosh, A. R.Emerging concepts for the dynamical organization of resting-state activity in the brain. Nat. Rev. Neurosci. 12(1), 43–56 (2011).

D'Angelo, E., & Jirsa, V. The quest for multiscale brain modeling. Trends Neurosci. (2022).

Friston, K. The free-energy principle: a unified brain theory?. Nat. Rev. Neurosci. 11(2), 127-138 (2010).

Ghosh, A., Rho, Y., McIntosh, A. R., Kötter, R., & Jirsa, V. K. Noise during Rest Enables the Exploration of the Brain's Dynamic Repertoire. PLoS Comput. Biol. 4(10), (2008).

Ittner, L. M. et al. Dendritic function of tau mediates amyloid-β toxicity in Alzheimer's disease mouse models. Cell. 142, 387–397 (2010).

Patow, G., Stefanovski, L., Ritter, P., Deco, G., & Kobeleva, X. Whole-brain modeling of the differential influences of Amyloid-Beta and Tau in Alzheimer's Disease. bioRxiv. (2022).

Roberson, E. D. et al. Reducing endogenous tau ameliorates amyloid β -induced deficits in an Alzheimer's disease mouse model. Science. 316, 750–754 (2007).

Sachdev, P. S., Brodaty, H., Reppermund, S., Kochan, N. A., Trollor, J. N., Draper, B., Slavin, M. J., Crawford, J., Kang, K., Broe, G. A., & Others. (2010). The Sydney Memory and Ageing Study (MAS): methodology and baseline medical and neuropsychiatric characteristics of an elderly epidemiological non-demented cohort of Australians aged 70–90 years. International Psychogeriatrics / IPA, 22(8), 1248–1264.

Sanz Leon, P., Knock, S. A., Woodman, M. M., Domide, L., Mersmann, J., McIntosh, A. R., & Jirsa, V. The Virtual Brain: A simulator of primate brain network dynamics. Front. Neuroinform. 7 (2013).

Stefanovski, L., Triebkorn, P., Spiegler, A., Diaz-Cortes, M. A., Solodkin, A., Jirsa, V., … & Alzheimer's Disease Neuroimaging Initiative. Linking molecular pathways and large-scale computational modeling to assess candidate disease mechanisms and pharmacodynamics in Alzheimer's disease. Front. Comput. Neurosci. 13, 54 (2019).

Triebkorn, P., Stefanovski, L., Dhindsa, K., Diaz-Cortes, M. A., Bey, P., Bülau, K., … & Alzheimer's Disease Neuroimaging Initiative. Brain simulation augments machine-learning–based classification of dementia. Alzheimer's & Dement.: Transl. Res. Clin. Interv. 8(1), e12303 (2022).

Tsang, R. S. M., Sachdev, P. S., Reppermund, S., Kochan, N. A., Kang, K., Crawford, J., Wen, W., Draper, B., Trollor, J. N., Slavin, M. J., Mather, K. A., Assareh, A., Seeher, K. M., & Brodaty, H. (2013). Sydney Memory and Ageing Study: an epidemiological cohort study of brain ageing and dementia. International Review of Psychiatry, 25(6), 711–725.

Yalçınkaya, B. H., Ziaeemehr, A., Fousek, J., Hashemi, M., Lavanga, M., Solodkin, A., McIntosh, A. R., Jirsa, V. K., & Petkoski, S. (2023). Personalized virtual brains of Alzheimer's Disease link dynamical biomarkers of fMRI with increased local excitability. In bioRxiv.

Zimmermann, J., Perry, A., Breakspear, M., Schirner, M., Sachdev, P., Wen, W., … & Solodkin, A. Differentiation of Alzheimer's disease based on local and global parameters in personalized Virtual Brain models. NeuroImage: Clin. 19, 240-251 (2018).

Zimmermann, J., Perry, A., Breakspear, M., Schirner, M., Sachdev, P., Wen, W., … & Solodkin, A. Differentiation of Alzheimer's disease based on local and global parameters in personalized Virtual Brain models. NeuroImage: Clin. 19, 240-251 (2018).